

Non-equilibrium distributions at finite noise intensities

A. Bandrivskyy, S. Beri, D. G. Luchinsky[†]

Department of Physics, Lancaster University, Lancaster LA1 4YB, UK

(Dated: November 29, 2018)

We analyse the non-equilibrium distribution in dissipative dynamical systems at finite noise intensities. The effect of finite noise is described in terms of topological changes in the pattern of optimal paths. Theoretical predictions are in good agreement with the results of numerical solution of the Fokker-Planck equation and Monte Carlo simulations.

PACS numbers: 05.40.+j, 02.50.-r, 05.20.-y

The analysis of the probability distribution in systems away from thermal equilibrium is one of the main themes in statistical physics [1, 2] which has recently attracted renewed interest in the context of stochastic resonance [3] and stochastic ratchets [4]. Despite its importance, the theory of the probability distributions in non-equilibrium systems is still in its infancy.

One of the keys to the solution of this problem is an understanding of how a non-equilibrium system deviates far away from a steady state [1]. The probability of such deviations is small and can be approximated by a Boltzmann-like distribution of the form [5, 6]

$$\rho(x) = z(x) \exp(-S(x)/\epsilon), \quad \epsilon \rightarrow 0. \quad (1)$$

Here the action function $S(x)$ plays the role of a non-equilibrium potential [7], $z(x)$ is a prefactor and ϵ is the noise intensity. The majority of earlier studies have been restricted to the analysis of zero noise limit. In this limit properties of $\rho(x)$ are determined by the properties of optimal paths that are deterministic trajectories along which the system moves in the course of large deviations [5, 6]. Accordingly, the pattern of optimal paths plays a fundamental role in the zero-noise-limit theory.

In “real life”, however, the noise intensity is always finite. Calculations of $\rho(x)$ at finite noise intensity, that allow for a direct comparison with an experiment, require analysis of the all-important *prefactor*. Such analysis has recently been initiated in a number of publications [8, 9, 10] dealing with the closely related problem of noise-induced *escape* over an unstable limit cycle.

The research has shown that one has “to leave room for the possibility that, even for small noise strengths ϵ , more than one” optimal path contributes significantly to the escape [9, 10]. However, this plausible assumption contradicts the fundamental properties of the pattern of optimal paths including the existence of the singularities and generic uniqueness of the most probable escape path (see e.g. [7, 11, 12]). This inconsistency does not allow the use of the methods of [8, 9, 10] to compute noise-induced variations of the non-equilibrium distribution in the *whole of phase space*. As mentioned in [10] the problem is “intricate” due to the subtle properties of the pattern of optimal paths near the basin boundary.

In this Letter, the $\rho(x)$ is calculated over the whole of phase space as a function of noise intensity. Specifically,

we address the intricate problem of the noise-induced changes in the pattern of optimal paths near the singularities and show that noise-induced variations of $\rho(x)$ are related to the shift of the singularities and of the most probable escape paths. The theoretical predictions are verified by Monte Carlo simulations and the numerical integration of the Fokker-Planck equation (FPE). In the boundary region we find the position of singularities analytically, and provide a more accurate calculation of the oscillating probability distribution discussed in the recent publications [8, 9, 10], and suggest an intuitively clear physical picture of these oscillations.

To see why the computation of the prefactor calls for the analysis of the noise-induced topological changes in the pattern of optimal paths, let us consider a Langevin equation of the form

$$\dot{x}_i = K_i(x) + \sqrt{\epsilon} \sigma_{ij} \xi_j(t) \quad i, j = 1, 2. \quad (2)$$

Here x_i are coordinates of a 2-dimensional dissipative system, $\xi_j(t)$ are Gaussian zero-mean uncorrelated sources of noise linearly mixed by a given noise matrix σ_{ij} , and ϵ is a small parameter of the theory.

The evolution of the probability density $\rho(x, t)$ for the system (2) is described by the FPE

$$\frac{\partial \rho}{\partial t} = \frac{\partial}{\partial x_i} \left(-\rho K_i + \frac{\epsilon}{2} \frac{\partial}{\partial x_j} [Q_{ij} \rho] \right), \quad (3)$$

where $Q = \sigma^T \sigma$ is a positively defined diffusion matrix.

To the leading order of approximation in ϵ , S satisfies [5, 6] a Hamilton-Jacobi equation for a classical action in the form $H(x, \nabla S) = 0$, where $H(x, p)$ is the Hamiltonian function equals $\frac{1}{2} Q_{ij} p_i p_j + K_i(x) p_i$. The pattern of extreme trajectories emanating from the stationary state of the system (2) is found by integrating Hamiltonian equations with appropriate initial conditions (see e.g. [5]), and the action is found as an integral along these trajectories

$$\dot{x}_i = K_i + Q_{ij} p_j, \quad \dot{p}_i = -\frac{\partial K_j}{\partial x_i} p_j, \quad \dot{S} = \frac{1}{2} Q_{ij} p_i p_j. \quad (4)$$

In general more than one trajectory can arrive at the same point x [12], but in the limit of $\epsilon \rightarrow 0$ the only trajectories contributing to the $\rho(x)$ are those that provide the global minimum of the action and form the pattern of *optimal paths*. As a result of global minimization

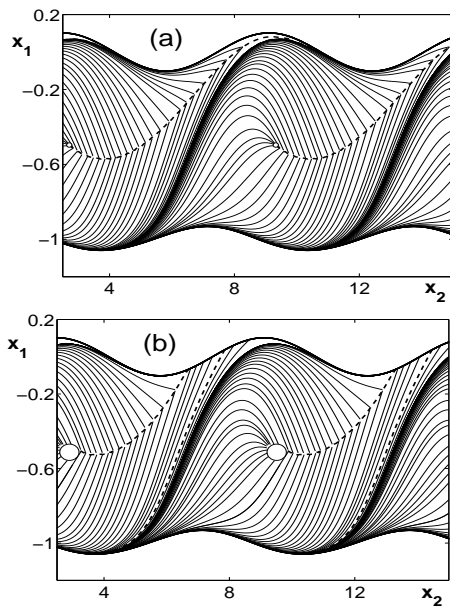


FIG. 1: The part of the pattern of optimal paths between the unstable and one of the stable limit cycles of a PDOD ($A = 0.1, \Omega = 2\pi$) (a) for $\epsilon = 0$ and (b) for $\epsilon = 0.015$. The stable $x_s(t)$ and unstable $x_u(t)$ limit cycles are shown by solid lines at the bottom and the top of the figure correspondingly. The empty region inside the circle is the “breakdown region” described in the text. The MPEP and the switching line are indicated by dashed lines.

the state space of 2-dimensional system (2) is separated by so-called *switching lines* into areas to which the system arrives along optimal paths of topologically different types [12]. In particular, the escape from a metastable state of the system (2) in the $\epsilon \rightarrow 0$ limit is governed by the properties of the so-called *most probable escape path* (MPEP) that emanates (at $t \rightarrow -\infty$) from a stationary state of (2) and arrives (at $t \rightarrow +\infty$) at the boundary of its basin of attraction. The pattern of optimal paths, switching line, and the most probable escape paths are shown in Fig. 1(a) for a periodically driven overdamped motion in a bistable Duffing (PDOD) system: $K_1 = x - x^3 + A \sin(\Omega t)$, $K_2 = \Omega = 2\pi/T$, $\sigma_{ij} = \sqrt{2}\delta_{i1}\delta_{j1}$ ($x_1 = x$ and $x_2 = \Omega t$).

The pattern is periodic in time and the behavior of the switching line and of the MPEP near the basin boundary is described by the scaling properties of the solution of the linearized Hamiltonian equations (c.f. [8, 9, 10, 13]) in a Poincaré section (see Fig. 2) in the form

$$p_n = y_0^* \cdot W_0 \cdot a^n, \quad (5)$$

$$y_n = y_0^* \cdot a^{-n} + p_n \cdot W_0, \quad (6)$$

where $y_n = x(t) - x_u(t)$ is the distance to the limit cycle at time $t = t_0 + nT$, $a = e^{-\lambda T}$, $\lambda = 1/T \int_t^{t+T} \partial_{x_1} K_1 dt'$, and $W_0 = (1 - a^2) \left[2 \int_t^{t+T} a^2(t', t) dt' \right]^{-1}$ is the second derivative of the action in the x direction ($W_0 = \partial_y \partial_y S$

see eq. (8) below).

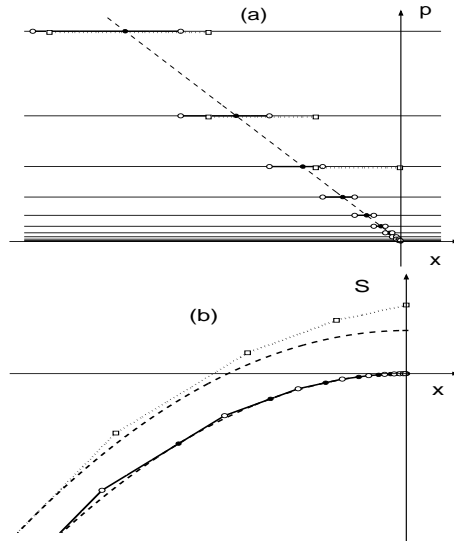


FIG. 2: (a) A section of the lagrangian manifolds. $\mathcal{M}_u^{(s)}$ is shown by the dashed line. $\mathcal{M}_s^{(u)}$ is a set of horizontal lines. Physically observable part of the $\mathcal{M}_s^{(u)}$ formed by the optimal paths is shown by the thick segments for $\epsilon = 0$ and by dashed segments for $\epsilon \neq 0$. The MPEP is shown by dots at the intersection of the two manifolds. The switching line is shown by the open circles for $\epsilon = 0$ and by squares for $\epsilon \neq 0$. (b) A section of the non-equilibrium potential (solid line). The MPEP is shown by dots where $S(y)$ touches the parabola (dashed line). The switching line corresponds to the points of singularities of $S(y)$ (open circles). The section of the modified action surface $S - \epsilon \ln z$ is shown by dotted line and shifted switching line (for $\epsilon \neq 0$) is shown by squares.

The first term in the RHS equation (6) describes the divergence of the zero-momentum trajectory from $x_u(t)$ corresponding to the motion on the unstable manifold of this cycle $\mathcal{M}_u^{(u)}$. The second term corresponds to the motion on the stable manifold $\mathcal{M}_s^{(s)}$ of $x_u(t)$ with non-zero momentum. We note that the initial position of the most probable escape path $y_0^* = x(t_0) - x_u(t_0)$ is the only global parameter of the linear problem. It defines the intersection of $\mathcal{M}_u^{(s)}$ and the unstable manifold of the stable limit cycle $\mathcal{M}_s^{(u)}$ (see Fig. 2(a)). The latter is a set of horizontal lines. The physically observable part of $\mathcal{M}_s^{(u)}$ formed by the optimal paths is a set of segments (see Fig. 2(a)) limited by the switching line.

The position of the switching line is found by noting that the cross-section of the action $S(y)$, as a function of the distance y from the cycle, is a piecewise linear approximation of an ideal parabola $S_{esc} - \frac{1}{2}y^2 W_0$ [7, 10, 13], where S_{esc} is an escape action in zero-noise limit. The MPEP corresponds to the points where $S(y)$ touches the parabola. The switching line corresponds to the points of singularities of $S(y)$.

It follows from this geometrical picture that at $\epsilon = 0$: (i) MPEP is the only optimal path that approaches the

unstable limit cycle at $t \rightarrow \infty$, (ii) the position of the switching line scales as $y_n^{sl} = (a+1)y_0^*a^n/2$ and (iii) the switching line also approaches the unstable limit cycle at $t \rightarrow \infty$ in agreement with the qualitative picture shown in Fig. 1(a). A similar picture can be obtained for the inverted van der Pol oscillator (see [10](b)) and is generic for 2D systems with unstable limit cycles.

In the presence of the finite noise intensity, this picture breaks down. As we have mentioned above, one has to assume that, even for small noise intensity, more than one trajectory contributes significantly to the probability of crossing the boundary [9]. The choice of a *right* set of trajectories that cross the boundary is a subtle problem [10] owing to the fact [7] that extreme trajectories intersect one another wildly near the unstable limit cycle. For example, in [8] a contribution to the escape from *all* the trajectories that emanate from the steady state is estimated analytically. In [9, 10] it was suggested that the main contribution to the escape comes from an *infinite discrete set* of trajectories that are small perturbations of the MPEP, which is found numerically. Neither of these choices is consistent with the existence of the switching line, and the methods of [8, 9, 10] cannot be applied to compute noise-induced variation of the $\rho(x)$ over the whole of phase space (cf. [14]).

We therefore suggest that, to analyze the distribution in the whole phase space, it is necessary to investigate the noise-induced changes in the pattern of optimal paths. Such an analysis can be conveniently performed in the next-to-leading order of approximation in ϵ of the solution of the FPE, yielding [5] an equation for the prefactor in (1) and for the Hessian matrix $S_{ij} \equiv \partial_i \partial_j S$ [15]

$$\frac{dz}{dt} = -z \left(\partial_i K_i + \frac{1}{2} Q_{ij} S_{ij} \right), \quad (7)$$

$$\begin{aligned} \dot{S}_{ij} &= -p_m \partial_i \partial_j K_m - S_{im} \partial_j K_m \\ &\quad - S_{jm} \partial_i K_m - S_{jm} S_{ik} Q_{km}. \end{aligned} \quad (8)$$

The second derivative of the action vanishes rapidly near $x_u(t)$ on $\mathcal{M}_s^{(u)}$, corresponding to the fact that $\mathcal{M}_s^{(u)}$ is a set of horizontal lines near $x_u(t)$. Therefore (for the PDOD) the noise induced correction to the action $-\epsilon \ln(z(t))$ over one period can be estimated as $\epsilon \lambda T$. As a result, a straightforward application of the equations (4), (7), (8) leads to a discontinuity in the probability distribution at the position of the switching line of size $\epsilon \lambda T$.

This discontinuity is unphysical. It can be removed if one defines the position of a generalized switching line as a set of points: $z_1 \cdot \exp(-S_1/\epsilon) = z_2 \cdot \exp(-S_2/\epsilon)$ for which *probabilities* of arrival along topologically different optimal paths are equal. We note that this is a natural generalization of the original definition [12] and the latter is recovered when ϵ goes to zero. It has physical significance of being the locus of experimentally observable points where the curvature of the probability distribution undergoes sharp qualitative changes (cf. [16]). The noise-induced changes in the physically observable part of the

$\mathcal{M}_s^{(u)}$ and in the $-\epsilon \ln \rho(x)$ are shown in Fig. 2. Note the overall shift of the $-\epsilon \ln \rho(x)$ due to the prefactor, and a stepwise shifts of the linear segments by $\epsilon \lambda T$ without the change of their slope. The geometrical analysis of these changes gives the position of the modified switching line in the form $y_n^{sl} = (a+1)y_n/2 - \epsilon T W_0 / ((1-a)y_n)$.

The change in the position of the switching line has profound consequences for the analysis of the non-equilibrium distribution and the escape problem for the finite noise intensities. Firstly, $\rho(x, t)$ calculated in the next to the leading order of WKB approximation is now continuous everywhere in phase space. Secondly, the modified switching line has to shift “up” (compare Fig. 1 and Fig. 2), and for the linear regime it crosses the boundary at the point where the distance from the original MPEP to the boundary is $y_n^{(cr)} = \sqrt{2\epsilon T W_0 / (1-a^2)}$. Since the new switching line crosses the boundary, infinitely many optimal paths can now cross the boundary. Moreover, the original MPEP ceases to be the most probable escape path for a finite noise intensity, since it is now “cut off” by the intersection with the new switching line. Its role is taken by a different path that crosses the boundary. Furthermore, the dominant contribution to the escape from a metastable state is now governed by the continuous set of trajectories which arrive to the boundary through a “corridor” between the modified switching line and the original MPEP. The modified pattern of optimal paths, including the modified MPEP and the modified switching line, are shown in Fig. 1(b). For small noise intensities, the set of optimal trajectories that cross the boundary can be treated as small perturbations of the original MPEP.

We note that the values of the prefactor z and the Hessian computed along the paths diverge as a trajectory approaches a caustic. The approximation (7), (8) breaks down here, and the method described in this paper cannot be applied. The size of the breakdown region scales as $O(\epsilon^{2/3})$ near caustic and as $O(\epsilon^{3/4})$ near cusp (see e.g. [12, 15, 17]). Near the singularities $\rho(x)$ can be calculated using the Maslov-WKB approximation (see e.g. [12, 15]). The results of these calculations should merge in the “far field” the approximation found by the method described above. However, in practice, when calculating $S - \epsilon \ln(z)$ using eqs. (4), (7), (8), the problem of divergence can be avoided by partitioning the state space into boxes with the size that scales as $\epsilon^{2/3}$ and by assigning to each box the probability which is maximized over the set of trajectories that pass through this box.

To verify theoretical predictions we have performed Monte Carlo simulations and numerical integration of the FPE for two model systems: the PDOD and the inverted van der Pol oscillator $K_1 = x_2$, $K_2 = -x_1 - 2\eta x_2(1-x_1^2)$, $\sigma_{ij} = \sqrt{4\eta} \delta_{i2} \delta_{j2}$. Qualitatively similar behavior was obtained for both systems. In Fig. 3(a,b) we compare theoretical predictions for the function $S - \epsilon \ln(z)$ with the results of numerical calculations for the PDOD in different cross-sections. Both numerical techniques produce the same results and they are in good

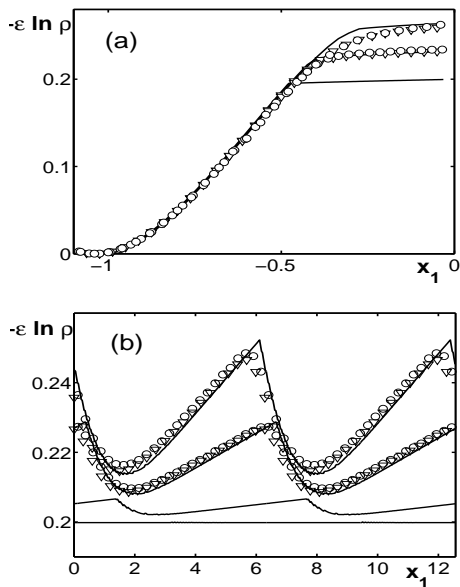


FIG. 3: (a) Sections at $x_1 = 4.1$ of the $-\epsilon \ln \rho(x)$ calculated (solid lines) for different values of ϵ (from the top to the bottom): 0.02, 0.01, 0. The results of the Monte Carlo simulations (circles) and solution of the FPE (triangles) for $\epsilon = 0.02$ (top) and 0.01 (bottom) are shown for comparison. (b) The $-\epsilon \ln \rho(x)$ calculated (solid lines) along the unstable limit cycle $x^{(u)}$ for four values of ϵ , from the top to the bottom, 0.01, 0.005, 0.001, and 0 are compared with Monte Carlo simulations (circles) and numerical solution of the FPE (triangles) for $\epsilon = 0.01$ (top) and 0.005 (bottom) respectively.

quantitative agreement with the theory for a wide range of noise intensity.

The behavior of $-\epsilon \ln(\rho(x))$ at the boundary on the metastable state is shown in Fig. 3(b) for various values of the noise intensity. It can be seen that the amplitude of

the finite-noise induced oscillations increases with ϵ . The maxima of these oscillations correspond to the intersection of the boundary with the modified switching line and are the nondifferentiability points of the modified action surface $S - \epsilon \ln(z)$. The minima of the distribution correspond to the intersection of the boundary by the modified MPEP, and in the linear regime are shifted with respect to the maxima by $\Delta t \approx \ln[2\lambda T/(1 - a_0^2)]/2\lambda$. For arbitrary values of parameters the position of the modified switching line and MPEP found in simulations coincide with those predicted theoretically. As the noise intensity ϵ decreases, the pattern of optimal paths and the modified action approach their zero-noise limits.

In conclusion, we have shown that the structure of singularities of non-equilibrium potential in the zero-noise limit can be modified in a self consistent way to include the effect of finite noise intensity. As a result, a simple numerical scheme can be used to calculate $\rho(x)$ over the whole of phase space in good quantitative agreement with the results of simulations and numerical integration of the FPE for two systems: inverted van der Pol and periodically driven overdamped Duffing oscillators.

In the boundary layer we find analytically the position of the modified switching line and modified MPEP, and give an intuitively clear physical interpretation to the oscillations of the probability at the boundary discussed in recent publications [8, 9, 10]. In particular, these results suggest that the oscillations of the escape rate as a function of the noise intensity predicted in [10] cannot be observed. The method suggested in this Letter can readily be extended to higher dimensional systems.

The work was supported by the Engineering and Physical Sciences Research Council (UK), the Joy Welch Trust (UK), the Russian Foundation for Fundamental Science, and INTAS.

-
- [1] L. Onsager and S. Machlup, *Phys. Rev.* **91**, 1505 (1953).
 [2] H. Haken, *Review of Modern Physics.* **47**, 67 (1975).
 [3] C. Nicolis, *Tellus* **34**, 1 (1982).
 [4] M. I. Dykman, H. Rabitz, V. N. Smelyanskiy, and B. E. Vugmeister, *Phys. Rev. Lett.* **79**, 1178 (1997); P. Jung, J. G. Kissner, and P. Hänggi, *Phys. Rev. Lett.* **76**, 3436 (1996).
 [5] D. Ludwig, *SIAM Rev.* **17**, 605 (1975).
 [6] M. Freidlin and A. D. Wentzel, *Random Perturbations in Dynamical Systems* (Springer, New-York, 1984).
 [7] R. Graham and T. Tel, *Phys. Rev. Lett.* **52**, 9 (1984).
 [8] V. N. Smelyanskiy, M. I. Dykman, and B. Golding, *Phys. Rev. Lett.* **82**, 3193 (1999); V. N. Smelyanskiy *et al.*, *J Chem. Phys.* **110**, 11488 (1999).
 [9] J. Lehmann, P. Reimann, and P. Hänggi, *Phys. Rev. Lett.* **84**, 1639 (2000); J. Lehmann, P. Reimann, and P. Hänggi, *Phys. Rev. E* **62**, 6282 (2000).
 [10] (a) R. S. Maier and D. L. Stein, *Phys. Rev. Lett.* **86**, 3942 (2001); (b) R. S. Maier and D. L. Stein, *Phys. Rev. Lett.* **77**, 4860 (1996).
 [11] H. R. Jauslin, *Physica A* **144**, 179 (1987).
 [12] M. I. Dykman, M. M. Millonas, and V. N. Smelyanskiy, *Phys. Lett. A* **195**, 53 (1994).
 [13] V. N. Smelyanskiy, M. I. Dykman, and R. S. Maier, *Phys. Rev. E* **55**, 2369 (1997).
 [14] A. Bandrivskyy, D. G. Luchinsky, and P. V. E. McClintock, *Phys. Rev. E* **66**, 021108 (2002).
 [15] R. S. Maier and D. L. Stein, *SIAM J. Appl. Math.* **57**, 752 (1997).
 [16] D. G. Luchinsky and P. V. E. McClintock, *Nature* **389**, 463 (1997); D. G. Luchinsky, P. V. E. McClintock, and M. I. Dykman, *Reports on Progress in Physics* **61**, 889 (1998).
 [17] L. Schulman, *Techniques and applications of path integration* (Wiley, New York, 1981).